Asymmetrical Gauss–Hermite Beam-Mode Analysis of the Hexagonal Horn

Tao Shen, *Student Member, IEEE*, Wenbin Dou, *Member, IEEE*, and Zhongliang Sun

***Abstract*— *Asymmetrical* Gauss–Hermite beam-mode analysis is presented to investigate the hexagonal horn. The fractional power in the fundamental beam mode is approximately 86%. The near- and far-field radiation patterns are calculated. The high fractional power in the fundamental beam mode of the horn indicates that it can be used as an efficient Gaussian beam launcher in quasi-optical systems.**

***Index Terms*— Horn antennas.**

I. Introduction

At MILLIMETER and submillimeter waves, conventional guided-wave techniques (such as waveguides) become increasingly difficult to apply due to the decreasing dimensions and increasing losses of the components. These problems can be overcome entirely or partly by using quasi-optical techniques, in which radiating beams propagate unguided, but effectively confined near a propagation axis from one beam-forming component to another in free space.

The behavior of quasi-optical systems is almost universally investigated by means of Gaussian beam-mode analysis [1], [2]. Gaussian beam modes are approximate solutions to the wave equation, which appear in the form of Gauss–Hermite polynomials in rectangular coordinates or Gauss–Laguerre polynomials in cylindrical coordinates. Typically, only the fundamental beam mode is employed in Gaussian beam-mode analysis for quasi-optical system design. Clearly, the accuracy of analysis based on the fundamental Gaussian beam mode depends on the extent to which the fundamental beam mode can be launched from the guided-wave structure using so-called feed horns. Thus, in quasi-optical systems, a high-efficiency Gaussian beam launcher is a critical element for coupling to guided-wave devices such as mixers and detectors.

Gaussian beam-mode analysis of different types of feed horns used at millimeter waves and submillimeter waves has been studied by many researchers: the conical corrugated horn by Wylde [3], the uniformly illuminated aperture by Padman *et al.* [4], the conical smooth-walled horn by Murphy [5], the diagonal horn by Withington and Murphy [6] and Johansson and Whyborn [7], and the corrugated pyramidal square horn with corrugations in the E-plane walls by Shen *et al.* [8]. The results of the fundamental Gaussian beam-mode analysis for some commonly used types of feed horns are summarized in [9].

Although the conical corrugated horn [3] and corrugated pyramidal square horn with corrugations in the E-plane walls [8] launch an almost perfect Gaussian beam (the fractional power in the fundamental beam mode of these two types of horns is approximately 98%), they suffer from the difficulty and expensiveness of fabrication at millimeter waves, which become more prominent at submillimeter waves. Therefore, a number of alternatives to them have been proposed and investigated, among which the diagonal horn [6], [7] seems to be most attractive. The main advantage of the diagonal horn is the ease with which it can be fabricated using split block techniques, which have found wide employment in the fabrication of diverse millimeter- and submillimeter-wave waveguide circuits. In addition, the high-packing density, which can be achieved in an array, also makes the diagonal horn an attractive candidate for focal-plane imaging applications. Recently, a new type of horn—the hexagonal horn—has been proposed and investigated by Shen *et al.* [10]. Like the diagonal horn, the hexagonal horn also possesses the advantages of ease of fabrication and high-packing density.

In all of investigations of the above-mentioned different types of feed horns, (*symmetrical*) Gaussian beam-mode analysis was used. However, for feed horns with asymmetrical-aperture field distribution and/or aperture dimensions, e.g., the hexagonal horn (its E- and H-plane aperture widths are different) discussed in this paper, it is preferable to use asymmetrical Gaussian beam-mode (which has different beam parameters in the two orthogonal planes perpendicular to the propagation axis) analysis, which would increase the fractional power in the fundamental beam mode. Here, the asymmetrical Gaussian beam mode is used to best fit the asymmetrical aperture field (at the horn aperture plane). Note that the asymmetrical Gaussian beam mode has elliptical symmetry, while the (symmetrical) Gaussian beam mode has circular symmetry. Since the beam parameters in the two orthogonal planes are independent, the asymmetrical Gaussian beam mode can be dealt with in a manner similar to the symmetrical one. Goldsmith [11] has pointed out that the asymmetrical Gaussian beam can be symmetrized by proper quasi-optical components such as cylindrical lenses. Recently, asymmetrical Gauss–Hermite beam-mode analysis has been presented to investigate the corrugated pyramidal rectangular horn with corrugations in the E-plane walls by Shen *et al.* [12].

In this paper, asymmetrical Gauss–Hermite beam-mode analysis is presented to investigate the hexagonal horn. The high fractional power in the fundamental beam mode of the

Manuscript received May 6, 1997; revised March 9, 1998.

T. Shen was with the State Key Laboratory of Millimeter Waves, Southeast University, Nanjing, Jiangsu 210096, China. He is now with the Department of Electrical Engineering, University of Maryland at College Park, College Park, MD 20742 USA.

W. Dou and Z. Sun are with the State Key Laboratory of Millimeter Waves, Southeast University, Nanjing, Jiangsu 210096, China.

Publisher Item Identifier S 0018-9480(98)07243-3.

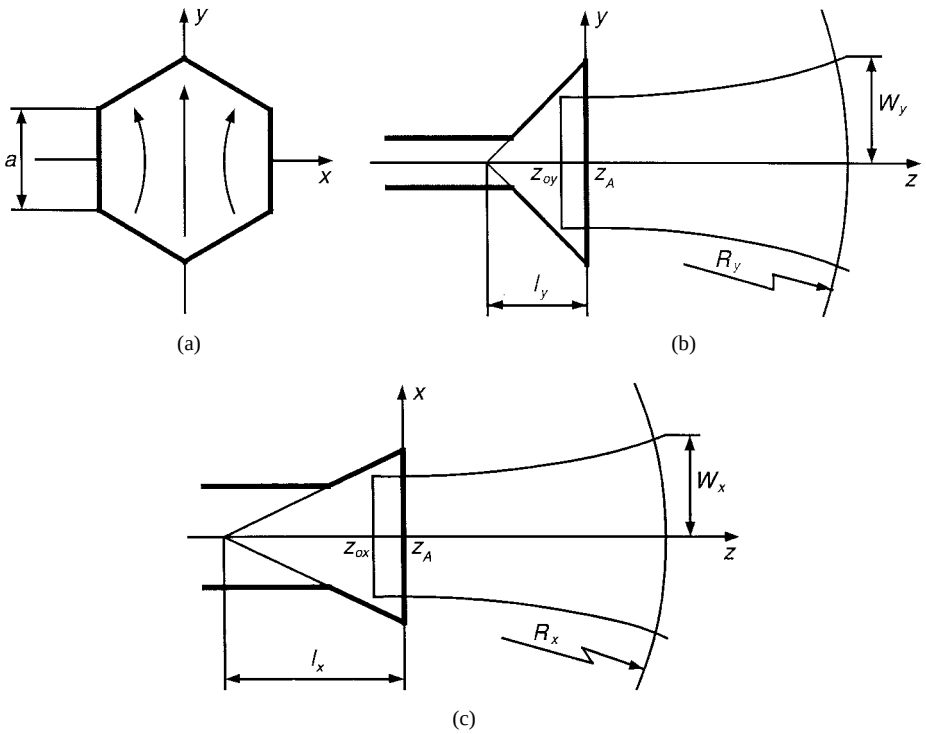

Fig. 1. Horn geometry. (a) Front view. (b) E-plane cut view. (c) H-plane cut view.

horn, which is slightly higher than the result for the diagonal horn, indicates that it can be used as an efficient Gaussian beam launcher in quasi-optical systems.

II. Asymmetrical Guass–Hermite Beam-Mode Model

For the diagonal horn, the aperture field is assumed to be composed of two equiamplitude and inphase TE_{10} modes crossing at an angle of 90° (i.e., they are orthogonal) [6], [7], [13]. Similarly, for the hexagonal horn, the aperture field can be assumed to be composed of two equiamplitude and inphase TE_{10} modes crossing at an angle of 60° [10]. Thus, referring to Fig. 1, the electric-field distribution at the hexagonal horn aperture plane can be approximated by (1), shown at the bottom of this page, where

$$\prod(x, y) = \begin{cases} 1, & \text{if } \left|\sqrt{3}y \pm x\right| \le \sqrt{3} \text{ and } |x| \le \dfrac{\sqrt{3}}{2} \\ 0, & \text{otherwise} \end{cases} \quad (2)$$

E_o is an arbitrary constant, a is the side length of the horn aperture, $k = 2\pi/\lambda$ is the free-space wavenumber, λ is the free-space wavelength, z_A is the location at which the horn aperture plane lies, and l_x and l_y are the distances from the imaginary apexes to the horn aperture plane along the z-axis in the H- and E-planes, respectively. The phase term $\exp(-jkz_A)$ in (1) has no meaning, except to make the unknown beam-mode coefficients A_{mn} and B_{mn} real, which will be given later. The electric-field distribution at the horn aperture plane given here is more general than that in [10], where the imaginary apexes in the H- and E-planes were assumed to be coincident, i.e., $l_x = l_y$.

The co-polarized (y-directed) electric-field distribution at the horn aperture plane is symmetrical with respect to both x- and y-axes, whereas the cross-polarized (x-directed) electric-field distribution at the horn aperture plane is antisymmetrical with respect to both x- and y-axes. Therefore, the horn has no boresight cross-polarization. In addition, the magnitude of the cross-polarized electric field at the horn aperture is $\sqrt{3}$ times less than the magnitude of the co-polarized electric field at the horn aperture. The polarization efficiency is

$$\begin{aligned} \eta_{\mathrm{p}} &= \frac{P_{\mathrm{co}}}{P_{\mathrm{tot}}} = \frac{P_{\mathrm{co}}}{P_{\mathrm{co}} + P_{\mathrm{cr}}} \\ &= \frac{\displaystyle\int_{-\infty}^{\infty}\int_{-\infty}^{\infty} |E_y(x, y, z_A)|^2 dx\, dy}{\displaystyle\int_{-\infty}^{\infty}\int_{-\infty}^{\infty} \left[|E_y(x, y, z_A)|^2 + |E_x(x, y, z_A)|^2\right] dxdy} \\ &= \frac{84 + 27\pi^2}{40 + 36\pi^2} \\ &= 88.66\% \end{aligned} \quad (3)$$

$$\begin{aligned} \bar{E}(x, y, z_A) &= \hat{y}E_y(x, y, z_A) + \hat{x}E_x(x, y, z_A) \\ &= E_o\left[\hat{y}\cos\left(\frac{\pi x}{\sqrt{3}a}\right)\cos\left(\frac{\pi y}{2a}\right) + \hat{x}\frac{1}{\sqrt{3}}\sin\left(\frac{\pi x}{\sqrt{3}a}\right)\sin\left(\frac{\pi y}{2a}\right)\right]\prod\left(\frac{x}{a}, \frac{y}{a}\right)\exp\left(-jkz_A - j\frac{\pi x^2}{\lambda l_x} - j\frac{\pi y^2}{\lambda l_y}\right) \end{aligned} \quad (1)$$

where $P_{\rm tot}$, $P_{\rm co}$, and $P_{\rm cr}$ denote the total, co-, and cross-polarized powers, respectively. The cross-polarized power could be eliminated by polarizer grids, which results in a polarization loss of approximately 0.523 dB.

The aperture field must be somehow excited. For the diagonal horn, Love [13] used a section of circular waveguide as a transition from standard rectangular waveguide, while Johansson and Whyborn [7] used a more simple *direct* transition. Due to the aperture field resemblance between the hexagonal horn and the diagonal horn, it seems reasonable to believe that both kinds of transitions used for the diagonal horn are applicable to the hexagonal horn.

Since the aperture dimensions are not symmetrical, the field radiated from the horn are represented as a sum of asymmetrical Gauss–Hermite beam modes, as shown in (4), at the bottom of this page [2], [12], where A_{mn} and B_{mn} are the unknown co- and cross-polarized beam-mode coefficients to be determined later, H_m is the Hermite polynomial of order m, W_x, and W_y are the mode-independent beam widths in the two orthogonal xoz- and yoz-planes, respectively (throughout this paper, subscripts x and y denote parameters in the xoz- and yoz-planes, i.e., H- and E-planes, respectively), which vary with z according to

$$W_{x,y}(z) = W_{ox,oy}\sqrt{1+\left(\frac{z-z_{ox,oy}}{z_{cx,cy}}\right)^2} \tag{5}$$

where z_{ox} and z_{oy} are the beam-waist locations at which W_x and W_y take their minimum values W_{ox} and W_{oy} (the beam-waist widths) in the xoz- and yoz-planes, respectively; z_{cx} and z_{cy} are the confocal distances in the xoz- and yoz-planes, respectively, which are defined by

$$z_{cx,cy} = \frac{\pi W_{ox,oy}^2}{\lambda} \tag{6}$$

R_x and R_y are the mode-independent radii of curvature of the wavefront in the xoz- and yoz-planes, respectively, which vary with z according to

$$R_{x,y}(z) = (z-z_{ox,oy})\left[1+\left(\frac{z_{cx,cy}}{z-z_{ox,oy}}\right)^2\right] \tag{7}$$

ϕ_x and ϕ_y are the phase slippages per beam mode in the xoz- and yoz-planes, respectively, which vary with z according to

$$\phi_{x,y}(z) = \tan^{-1}\left(\frac{z-z_{ox,oy}}{z_{cx,cy}}\right) \tag{8}$$

and ϕ_{ox} and ϕ_{oy} are arbitrary phase constants per beam mode in the xoz- and yoz-planes, respectively. In addition, W_{Ax} and W_{Ay} in (4) denote W_x and W_y at the horn aperture plane, respectively.

In order to make the beam-mode coefficients A_{mn} and B_{mn} in (4) real, R_x and R_y at the horn aperture plane (denoted by R_{Ax} and R_{Ay} hereafter, respectively) are set to be

$$R_{Ax,Ay} = R_{x,y}(z_A) = l_{x,y} \tag{9}$$

and the adjustable ϕ_{ox} and ϕ_{oy} are set to be

$$\phi_{ox,oy} = -\tan^{-1}\left(\frac{z_A - z_{ox,oy}}{z_{cx,cy}}\right). \tag{10}$$

Using the orthogonality property of Hermite polynomials, and after some manipulations, the beam-mode coefficients A_{mn} and B_{mn} can be determined by evaluating the overlap integral over the horn aperture plane, and are given by

$$\begin{aligned} A_{mn} = {} & \sqrt{\frac{6}{\pi 2^{m+n}m!n!}}\frac{2E_o}{(W_{Ax}/a)(W_{Ay}/a)} \\ & \times \int_0^1 \cos\left(\frac{\pi u}{2}\right) H_m\left[\frac{\sqrt{6}u}{2(W_{Ax}/a)}\right] \\ & \times \exp\left[\frac{-3u^2}{4(W_{Ax}/a)^2}\right] du \int_0^{1-u/2} \cos\left(\frac{\pi v}{2}\right) \\ & \times H_n\left[\frac{\sqrt{2}v}{(W_{Ay}/a)}\right] \exp\left[\frac{-v^2}{(W_{Ay}/a)^2}\right] dv \end{aligned} \tag{11}$$

$$\begin{aligned} B_{mn} = {} & \sqrt{\frac{2}{\pi 2^{m+n}m!n!}}\frac{2E_o}{(W_{Ax}/a)(W_{Ay}/a)} \\ & \times \int_0^1 \sin\left(\frac{\pi u}{2}\right) H_m\left[\frac{\sqrt{6}u}{2(W_{Ax}/a)}\right] \\ & \times \exp\left[\frac{-3u^2}{4(W_{Ax}/a)^2}\right] du \int_0^{1-u/2} \sin\left(\frac{\pi v}{2}\right) \\ & \times H_n\left[\frac{\sqrt{2}v}{(W_{Ay}/a)}\right] \exp\left[\frac{-v^2}{(W_{Ay}/a)^2}\right] dv. \end{aligned} \tag{12}$$

Equation (11), for the co-polarized beam-mode coefficients, is valid only when both m and n are even; otherwise, $A_{mn}=0$. Equation (12), for the cross-polarized beam-mode coefficients, is valid only when both m and n are odd; otherwise, $B_{mn}=0$.

The co- and cross-polarized fractional powers in the mnth beam mode are given by (13) and (14), shown at the bottom of the following page. Analogous to the case for A_{mn} and B_{mn}, (13) is valid only when both m and n are even; otherwise, the co-polarized fractional power in the mnth beam mode is equal to zero, whereas (14) is valid only when both m

$$\begin{aligned} \bar{E}(x,y,z) = {} & \sum_{m=0}^{\infty}\sum_{n=0}^{\infty}(\hat{y}A_{mn}+\hat{x}B_{mn})\sqrt{\frac{2W_{Ax}W_{Ay}}{\pi 2^{m+n}m!n!W_xW_y}}\,H_m\left(\frac{\sqrt{2}x}{W_x}\right)H_n\left(\frac{\sqrt{2}y}{W_y}\right) \\ & \times \exp\left[-\left(\frac{x}{W_x}\right)^2-\left(\frac{y}{W_y}\right)^2-jkz-j\frac{\pi x^2}{\lambda R_x}-j\frac{\pi y^2}{\lambda R_y}+j\left(m+\frac{1}{2}\right)(\phi_x+\phi_{ox})+j\left(n+\frac{1}{2}\right)(\phi_y+\phi_{oy})\right] \end{aligned} \tag{4}$$

TABLE I
THE BEAM-MODE COEFFICIENTS OF THE FIRST 42 (CO- AND CROSS-POLARIZED) ASYMMETRICAL GAUSS–HERMITE BEAM MODES AND THE FRACTIONAL POWER IN EACH BEAM MODE FOR $\xi_x = 0.597$ AND $\xi_y = 0.672$. THE FRACTIONAL POWERS IN THE REMAINING HIGHER ORDER CO- AND CROSS-POLARIZED BEAM MODES ARE 0.64% AND 1.93%, RESPECTIVELY. THE TOTAL FRACTIONAL POWERS IN THE CO- AND CROSS-POLARIZED BEAM MODES ARE 88.66% AND 11.34%, RESPECTIVELY

Mode		Coefficient	Fractional Power	Mode		Coefficient	Fractional Power
m	n	A_{mn}/E_o	P^{co}_{mn}/P_{tot}	m	n	B_{mn}/E_o	P^{cr}_{mn}/P_{tot}
0	0	1.434826	0.857841	1	1	0.421577	0.074056
0	2	0	0	1	3	-0.118131	0.005815
2	0	0	0	3	1	-0.002768	0.000003
0	4	-0.143458	0.008575	1	5	-0.030808	0.000395
2	2	-0.065357	0.001780	3	3	-0.072928	0.002216
4	0	-0.122572	0.006260	5	1	-0.070589	0.002076
0	6	0.068570	0.001959	1	7	0.070441	0.002068
2	4	0.004298	0.000008	3	5	0.064225	0.001719
4	2	0.028860	0.000347	5	3	0.070506	0.002071
6	0	0.047124	0.000925	7	1	0.024736	0.000255
0	8	0.004044	0.000007	1	9	-0.058366	0.001419
2	6	0.032501	0.000440	3	7	-0.024643	0.000253
4	4	0.018366	0.000141	5	5	-0.031845	0.000423
6	2	0.001162	0.000001	7	3	-0.019171	0.000153
8	0	0.013319	0.000074	9	1	0.020278	0.000171
0	10	-0.034876	0.000507	1	11	0.030996	0.000400
2	8	-0.034846	0.000506	3	9	-0.012455	0.000065
4	6	-0.026655	0.000296	5	7	-0.006713	0.000019
6	4	-0.014903	0.000093	7	5	-0.002387	0.000002
8	2	-0.012133	0.000061	9	3	-0.015305	0.000098
10	0	-0.030698	0.000393	11	1	-0.032991	0.000454

and n are odd; otherwise, the cross-polarized fractional power in the mnth beam mode is equal to zero. Therefore, the co- and cross-polarized beam modes are composed exclusively of beam modes of different order. The choice of the ratios W_{Ax}/a and W_{Ay}/a (denoted by ξ_x and ξ_y hereafter, respectively) is, in principle, arbitrary, but a logical choice is that which maximizes the fractional power in the fundamental (the lowest order, i.e., $m = 0$, $n = 0$) beam mode [3]. Using (13), the maximum fractional power in the fundamental beam mode—86%—is achieved for

$$\xi_x = \frac{W_{Ax}}{a} = 0.597 \tag{15}$$

$$\xi_y = \frac{W_{Ay}}{a} = 0.672. \tag{16}$$

Thus, the hexagonal horn has quite a high fundamental Gaussian beam-mode content, which is slightly higher than the result (84%) for the diagonal horn [6], [7]. Of course, due to the asymmetrical aperture dimensions, the horn discussed here launches the asymmetrical Gaussian beam, distinct from the symmetrical one which the diagonal horn launches. This is not a problem since the asymmetrical Gaussian beam can be symmetrized by proper quasi-optical components such as cylindrical lenses [11]. Compared with the result (85%) of (symmetrical) Gaussian beam-mode analysis [10], the fractional power in the fundamental beam mode given here does not obviously increase. This is because the difference between the E- and H-plane aperture widths of the hexagonal horn is not obvious. Table I lists the coefficients of the first 42 (co- and cross-polarized) beam modes and corresponding fractional powers for $\xi_x = 0.597$ and $\xi_y = 0.672$. It should be pointed out that the polarization efficiency—88.66%—has already been taken into account here (i.e., the fractional power in each beam mode is given in units of the total power). If only the co-polarized power is taken into account, the fractional power in the fundamental beam mode is as high as 97%. This point is meaningful because the fundamental beam mode itself is co-polarized and, as mentioned above, the cross-polarized power could be eliminated by polarizer grids.

Note that R_{Ax} and R_{Ay} have been set to be l_x and l_y, respectively (9), therefore, once ξ_x and ξ_y are known, the locations and the beam-waist widths in the xoz- and yoz-

$$\frac{P^{\rm co}_{mn}}{P_{\rm tot}} = \frac{W_{Ax}W_{Ay}A^2_{mn}}{\displaystyle\int_{-\infty}^{\infty}\int_{-\infty}^{\infty}\Big[|E_y(x,\,y,\,z_A)|^2 + |E_x(x,\,y,\,z_A)|^2\Big]\,dx\,dy} = \frac{6\sqrt{3}\pi^2}{10+9\pi^2}(W_{Ax}/a)(W_{Ay}/a)(A_{mn}/E_o)^2 \tag{13}$$

$$\frac{P^{\rm cr}_{mn}}{P_{\rm tot}} = \frac{W_{Ax}W_{Ay}B^2_{mn}}{\displaystyle\int_{-\infty}^{\infty}\int_{-\infty}^{\infty}\Big[|E_y(x,\,y,\,z_A)|^2 + |E_x(x,\,y,\,z_A)|^2\Big]\,dx\,dy} = \frac{6\sqrt{3}\pi^2}{10+9\pi^2}(W_{Ax}/a)(W_{Ay}/a)(B_{mn}/E_o)^2 \tag{14}$$

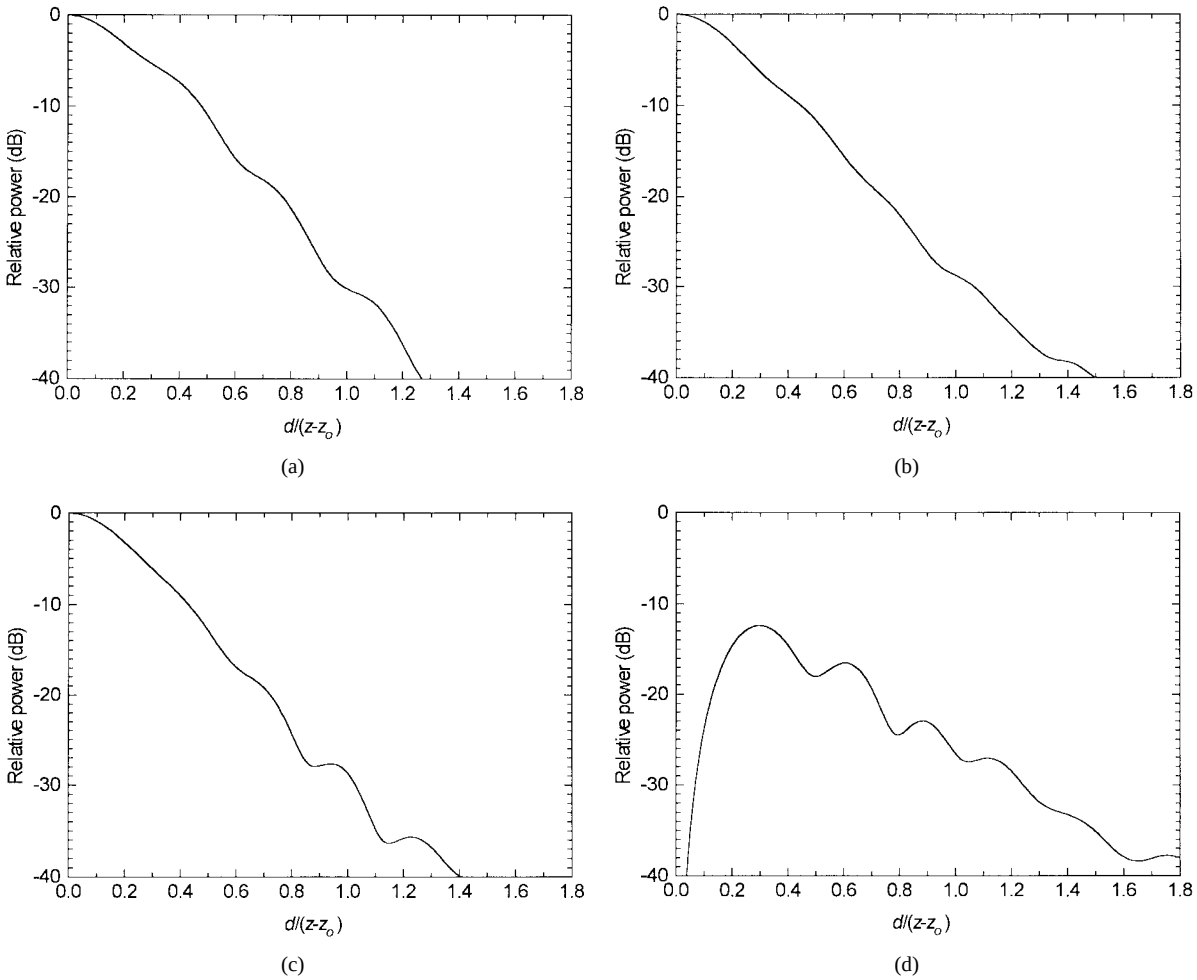

Fig. 2. Near-field radiation patterns. (a) Co-polarized E-plane. (b) Co-polarized H-plane. (c) Co-polarized D-plane. (d) Cross-polarized D-plane. The aperture dimension is $ka = 10$. 4/3 times the maximum phase change in the H-plane is $M_x/2\pi = 0.1$. The maximum phase change in the E-plane is $M_y/2\pi = 0.1$. The plane of interest is taken at $\hat{z} = 1$.

planes can be determined from (5) and (7), together with (6). The distances between the beam waists and the horn aperture along the z-axis are given by

$$z_A - z_{ox,\,oy} = \frac{l_{x,y}}{1 + \left(\dfrac{1}{\xi_{x,\,y}^2 M_{x,\,y}}\right)^2} \tag{17}$$

where

$$M_{x,\,y} = \frac{\pi a^2}{\lambda l_{x,\,y}} \tag{18}$$

are 4/3 times the maximum phase change in the H-plane and the maximum phase change in the E-plane, respectively, at the horn aperture, and the beam-waist widths are given by

$$W_{ox,\,oy} = \frac{\xi_{x,\,y} a}{\sqrt{1 + \left(\xi_{x,\,y}^2 M_{x,\,y}\right)^2}}. \tag{19}$$

In addition, the adjustable ϕ_{ox} and ϕ_{oy} become

$$\phi_{ox,\,oy} = -\tan^{-1}\left(\xi_{x,\,y}^2 M_{x,\,y}\right). \tag{20}$$

Thus, the beam parameters $W_{x,\,y}$, $R_{x,\,y}$, and $\phi_{x,\,y}$ at any plane of interest perpendicular to the propagation axis can be determined from (5), (7), and (8), together with (6). The field radiated from the horn can then be calculated from (4).

III. Near- and Far-Field Radiation Patterns

Taking the square of the absolute values of the co- and cross-polarized fields radiated from the horn given in (4), after some manipulations, the co- and cross-polarized near-field radiation patterns can be derived.

Fig. 2 shows the normalized co-polarized E-, H-, and D-planes, and cross-polarized D-plane near-field radiation patterns of the horn, as a function of $d/(z - z_o)$ for $ka = 10$, $M_x/2\pi = 0.1$, and $M_y/2\pi = 0.1$. The plane of interest is taken at $\hat{z} = 1$. $\hat{z}$ is defined by

$$\hat{z} = \frac{\hat{z}_x + \hat{z}_y}{2} \tag{21}$$

where

$$\hat{z}_{x,\,y}(z) = \frac{z - z_{ox,\,oy}}{z_{cx,\,cy}} \tag{22}$$

are the reduced distances in the xoz- and yoz-planes, respectively. Once $\hat{z}$ is given, $\hat{z}_x$ and $\hat{z}_y$ can be calculated

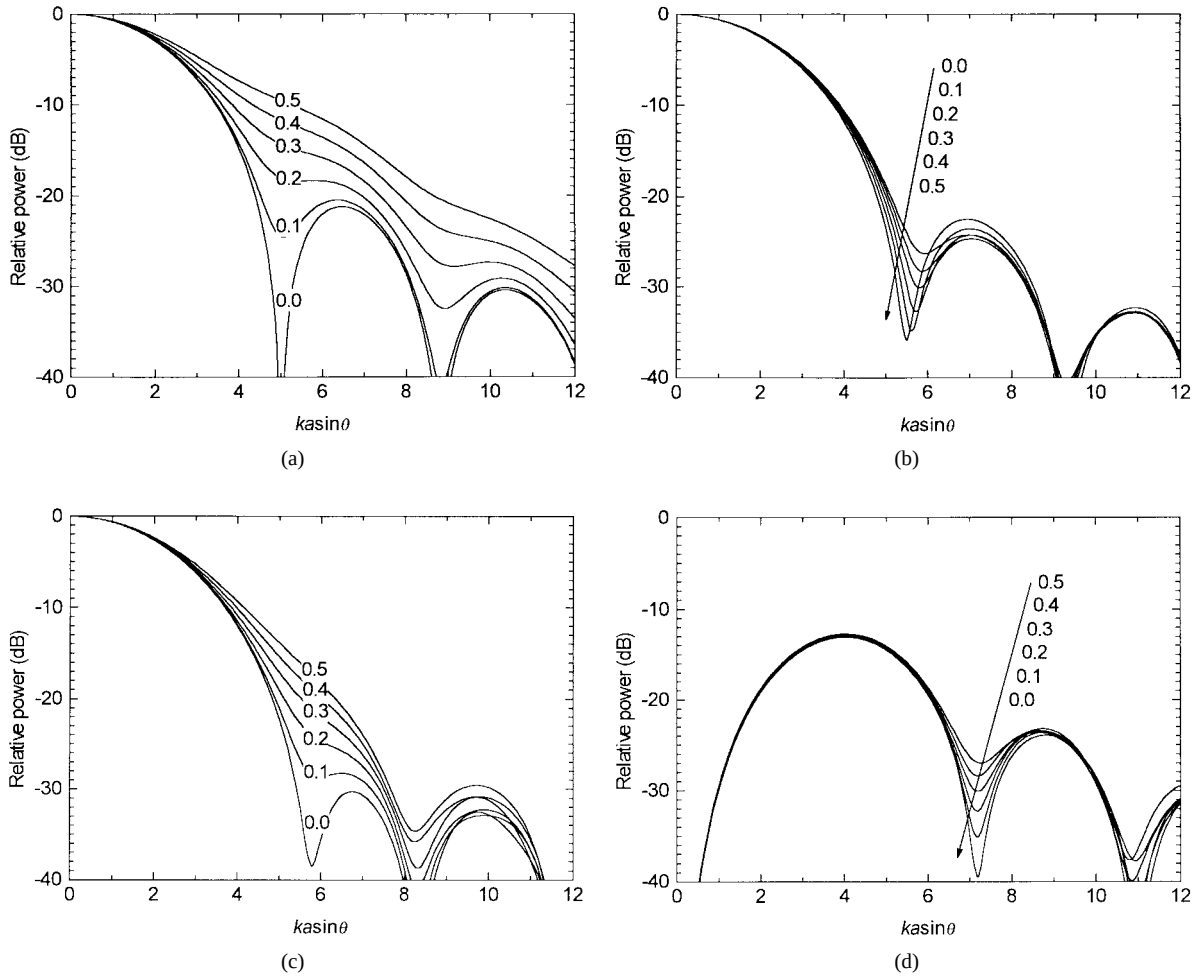

Fig. 3. Far-field radiation patterns. (a) Co-polarized E-plane. (b) Co-polarized H-plane. (c) Co-polarized D-plane. (d) Cross-polarized D-plane. 4/3 times the maximum phase change in the H-plane is $M_x/2\pi = 0.1$. Parameters are $M_y/2\pi$.

from

$$\hat{z}_x = \frac{z_{oy} - z_{ox} + 2z_{cy}\hat{z}}{z_{cx} + z_{cy}} \tag{23}$$

$$\hat{z}_y = \frac{z_{ox} - z_{oy} + 2z_{cx}\hat{z}}{z_{cx} + z_{cy}}. \tag{24}$$

d is the perpendicular distance from the z-axis. It is given in units of $z - z_o$, which is defined by

$$z - z_o = \frac{(z - z_{ox}) + (z - z_{oy})}{2} = \frac{z_{cx}\hat{z}_x + z_{cy}\hat{z}_y}{2}. \tag{25}$$

For the far-field,

$$\frac{z - z_{ox,\,oy}}{z_{cx,\,cy}} \to \frac{z - z_A}{z_{cx,\,cy}} \gg 1 \tag{26}$$

therefore,

$$W_{x,\,y}(z) \to \frac{W_{ox,\,oy}(z - z_A)}{z_{cx,\,cy}} = \frac{\lambda(z - z_A)}{\pi W_{ox,\,oy}}. \tag{27}$$

$$\phi_{x,\,y}(z) \to \frac{\pi}{2} \tag{28}$$

[see (5), (6), and (8)]. Using the transformation relationship between rectangular coordinates and spherical coordinates, the co- and cross-polarized far-field radiation patterns can then be derived, and are given by (29) and (30), shown at the bottom of the following page, where θ and φ are the off-boresight and azimuth angles, respectively.

Fig. 3 shows the normalized co-polarized E-, H-, and D-planes, and cross-polarized D-plane far-field radiation patterns of the horn as a function of $ka\sin\theta$ with $M_y/2\pi$ as a parameter for $M_x/2\pi = 0.1$. Fig. 4 shows the normalized co-polarized E-, H-, and D-planes, and cross-polarized D-plane far-field radiation patterns of the horn as a function of $ka\sin\theta$ with $M_x/2\pi$ as a parameter for $M_y/2\pi = 0.1$. It can be seen that M_x has an effect not only on H-plane radiation patterns, but also on E-plane radiation patterns, although its effect on E-plane radiation patterns is much less than on H-plane radiation patterns—so does M_y. This is due to the fact that the aperture of horn discussed in this paper is hexagonal. It is well known that when the radiating aperture is rectangular and its aperture field is separable in x and y, M_x (the maximum phase change in the H-plane) has no effect on the E-plane radiation patterns, and neither does M_y (the maximum phase change in the E-plane) on the H-plane radiation patterns.

In the near- and far-field radiation pattern calculation, beam modes from 00th to 40 40th are used. Gaussian beam-mode analysis converges slowly. As shown in Table I, even with

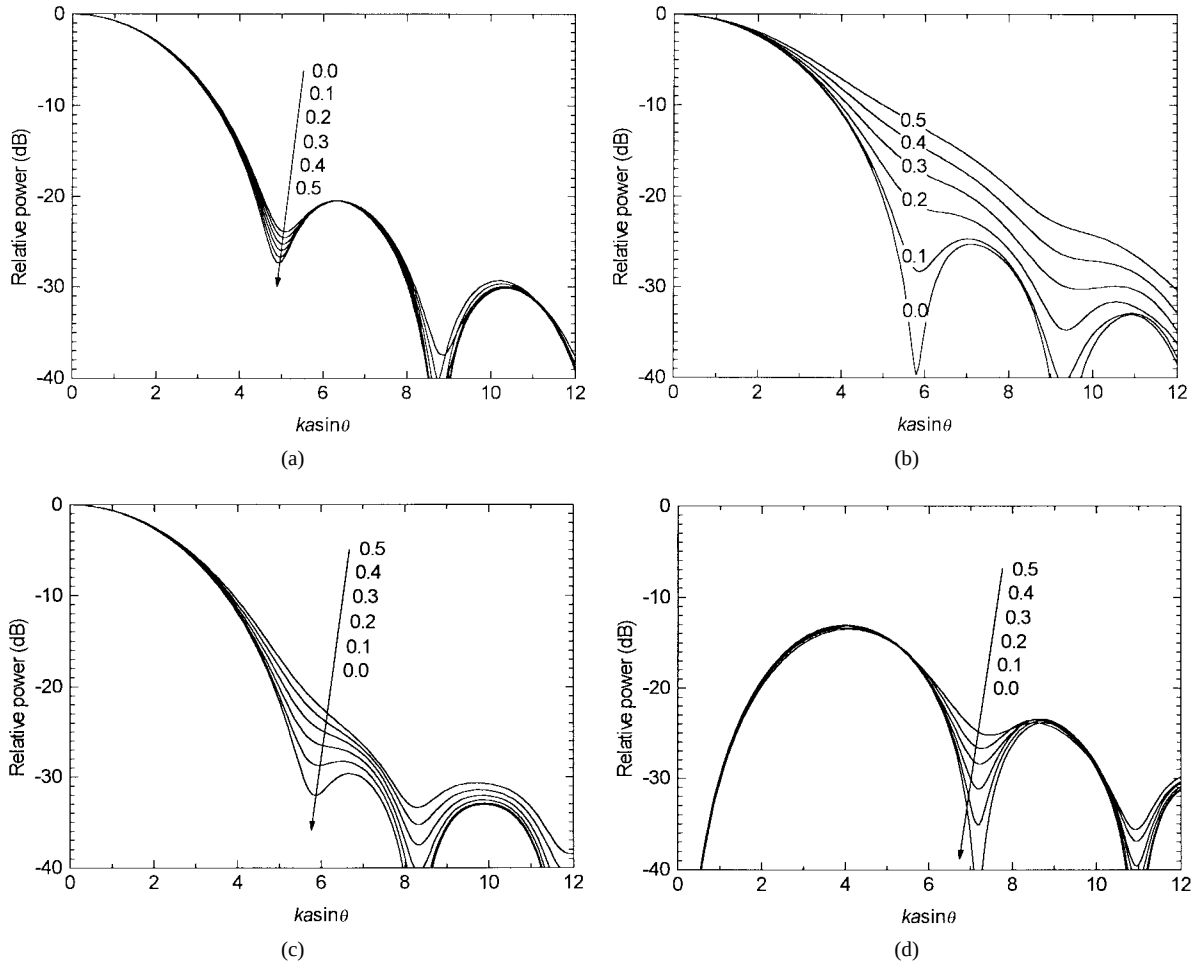

Fig. 4. Far-field radiation patterns. (a) Co-polarized E-plane. (b) Co-polarized H-plane. (c) Co-polarized D-plane. (d) Cross-polarized D-plane. The maximum phase change in the E-plane is $M_y/2\pi = 0.1$. Parameters are $M_x/2\pi$.

42 beam modes taken into account, there are still 0.64% co-polarized and 1.93% cross-polarized fractional powers unaccounted. The number of Gaussian beam modes needed in the radiation-pattern calculation depends on the sidelobe level being investigated, even if the fractional power in the fundamental beam mode is very high [8], [12]. In general, more beam modes are required to achieve greater accuracy in Gaussian beam-mode analysis.

$$P_{\mathrm{f}}^{\mathrm{co}}(\theta,\varphi) = \exp\left[-2\left(\frac{\pi W_{ox}}{\lambda}\tan\theta\cos\varphi\right)^2 - 2\left(\frac{\pi W_{oy}}{\lambda}\tan\theta\sin\varphi\right)^2\right] \times \left|\sum_{m=0}^{\infty}\sum_{n=0}^{\infty} A_{mn}\frac{1}{\sqrt{2^{m+n}m!n!}}H_m\left(\frac{\sqrt{2}\pi W_{ox}}{\lambda}\tan\theta\cos\varphi\right)H_n\left(\frac{\sqrt{2}\pi W_{oy}}{\lambda}\tan\theta\sin\varphi\right) \times \exp\left[j\left(m+\frac{1}{2}\right)\left(\frac{\pi}{2}+\phi_{ox}\right) + j\left(n+\frac{1}{2}\right)\left(\frac{\pi}{2}+\phi_{oy}\right)\right]\right|^2 \tag{29}$$

$$P_{\mathrm{f}}^{\mathrm{cr}}(\theta,\varphi) = \exp\left[-2\left(\frac{\pi W_{ox}}{\lambda}\tan\theta\cos\varphi\right)^2 - 2\left(\frac{\pi W_{oy}}{\lambda}\tan\theta\sin\varphi\right)^2\right] \times \left|\sum_{m=0}^{\infty}\sum_{n=0}^{\infty} B_{mn}\frac{1}{\sqrt{2^{m+n}m!n!}}H_m\left(\frac{\sqrt{2}\pi W_{ox}}{\lambda}\tan\theta\cos\varphi\right)H_n\left(\frac{\sqrt{2}\pi W_{oy}}{\lambda}\tan\theta\sin\varphi\right) \times \exp\left[j\left(m+\frac{1}{2}\right)\left(\frac{\pi}{2}+\phi_{ox}\right) + j\left(n+\frac{1}{2}\right)\left(\frac{\pi}{2}+\phi_{oy}\right)\right]\right|^2 \tag{30}$$

=

IV. Conclusion

Asymmetrical Gauss–Hermite beam-mode analysis has been presented to investigate the hexagonal horn. The fractional power in the fundamental beam mode is approximately 86%. The near- and far-field radiation patterns are calculated. The high fractional power in the fundamental beam mode of the hexagonal horn, which is slightly higher than the result for the diagonal horn, indicates that it can be used as an efficient Gaussian beam launcher in quasi-optical systems. The only distinction between the hexagonal horn and the diagonal horn is that the beam shape is different: the latter launches the (symmetrical) Gaussian beam, while the former launches the asymmetrical one. The asymmetrical Gaussian beam can be symmetrized by proper quasi-optical components such as cylindrical lenses [11], while the asymmetrical Gaussian beam may also be useful for illumination of special types of antennas, as well as in imaging applications, etc. Like the diagonal horn, the main advantage of the hexagonal horn is the ease with which it can be fabricated using split-block techniques. In addition, the high-packing density, which can be achieved in an array, also makes the hexagonal horn an attractive candidate for focal-plane imaging applications. Of course, the feasibility also depends on the degree of the coupling between the horns in an array. It should be pointed out that the fractional power in the fundamental beam mode of the hexagonal horn (approximately 86%) given in this paper is obtained based on the approximate electric-field distribution at the horn aperture plane. It seems reasonable to believe that its *actual* value is higher than the current one.

Acknowledgment

The authors would like to thank the anonymous reviewers for their helpful comments and suggestions.

References

[1] P. F. Goldsmith, "Quasioptical techniques at millimeter and submillimeter wavelengths," in *Infrared and Millimeter Waves,* vol. 6, K. J. Button, Ed. New York: Academic, 1982, ch. 5.

[2] J. C. G. Lesurf, *Millimeter-Wave Optics, Devices and Systems.* New York: Adam Hilger, 1990.

[3] R. J. Wylde, "Millimeter-wave Gaussian beam-mode optics and corrugated feed horns," *Proc. Inst. Elect. Eng.,* vol. 131, pt. H, no. 4, pp. 258–262, Aug. 1984.

[4] R. Padman, J. A. Murphy, and R. E. Hills, "Gaussian mode analysis of Cassegrain antenna efficiency," *IEEE Trans. Antennas Propagat.,* vol. AP-35, pp. 1093–1103, Oct. 1987.

[5] J. A. Murphy, "Aperture efficiencies of large axisymmetric reflector antennas fed by conical horns," *IEEE Trans. Antennas Propagat.,* vol. 36, pp. 570–575, Apr. 1988.

[6] S. Withington and J. A. Murphy, "Analysis of diagonal horns through Gaussian–Hermite modes," *IEEE Trans. Antennas Propagat.,* vol. 40, pp. 198–206, Feb. 1992.

[7] J. F. Johansson and N. D. Whyborn, "The diagonal horn as a submillimeter wave antenna," *IEEE Trans. Microwave Theory Tech.,* vol. 40, pp. 795–800, May 1992.

[8] T. Shen, W. Dou, and Z. Sun, "A new type of high efficiency Gaussian beam launcher," *J. Electromagn. Waves Applicat.,* vol. 11, pp. 145–156, 1997.

[9] P. F. Goldsmith, "Quasi-optical techniques," *Proc. IEEE,* vol. 80, pp. 1729–1747, Nov. 1992.

[10] T. Shen, Z. Sun, and W. Dou, "The hexagonal horn as an efficient Gaussian beam launcher," *IEEE Trans. Antennas Propagat.,* vol. 45, pp. 1173–1178, July 1997.

[11] P. F. Goldsmith, "Gaussian beam transformation with cylindrical lenses," *IEEE Trans. Antennas Propagat.,* vol. AP-34, pp. 603–607, Apr. 1986.

[12] T. Shen, Z. Sun, and W. Dou, "Asymmetrical Gauss–Hermite beam mode analysis of corrugated pyramidal rectangular horn," *Proc. Inst. Elect. Eng.,* vol. 143, no. 5, pt. H, pp. 385–389, Oct. 1996.

[13] A. W. Love, "The diagonal horn antenna," *Microwave J.,* vol. V, no. 3, pp. 117–122, Mar. 1962.

Tao Shen (S'95) was born in Suzhou, Jiangsu, China, on January 15, 1969. He received the B.S., M.S., and Ph.D. degrees in radio engineering from Southeast University, Nanjing, Jiangsu, China, in 1991, 1994, and 1997, respectively.

He is currently with the Department of Electrical Engineering, University of Maryland at College Park, College Park, MD.

Wenbin Dou (M'95) was born in Kunming, Yunnan, China, on July 8, 1954. He received the M.S. and Ph.D. degrees from the University of Electronics Science and Technology of China, Chengdu, Sichuan, China, in 1983 and 1987, respectively.

From 1987 to 1989, he worked as a Post-Doctoral Fellow at Southeast University, Nanjing, Jiangsu, China. Since 1989, he has been with the Department of Radio Engineering, Southeast University, where he is currently a Professor. He has authored and coauthored over 30 papers. His research interests include ferrite devices, millimeter-wave hybrid integrated circuits, and quasi-optical techniques.

Zhongliang Sun was born in Shanghai, China, in 1936. He graduated from the Department of Radio Engineering, Southeast University, Nanjing, Jiangsu, China, in 1960.

Since 1960, he has been with the Department of Radio Engineering, Southeast University, where he is currently a Professor and the Director of the State Key Laboratory of Millimeter Waves. From 1960 to 1977, he worked on low-noise microwave amplifiers, oscillators, and radar systems. From 1978 to 1986, his research activities involved millimeter-wave circuits and subsystems, including mixers, oscillators, power combiners, upconverters, receivers and transducers. Since 1987, his research interests have mainly included millimeter-wave integrated circuits and subsystems, phase-locking solid-state sources, optically controlled microwave circuits and devices, active feed-array antennas, wave polarizations, and ground-penetrating radars.